Supplementary Figures for "Addressing genetic tumor heterogeneity through computationally predictive combination therapy"

Boyang Zhao[1,2], Justin R. Pritchard[2,3,*], Douglas A. Lauffenburger[2,3,4,*] and Michael T. Hemann[2,3,*]

[1]Computational and Systems Biology Program, [2]The David H. Koch Institute for Integrative Cancer Research, [3]Department of Biology, and [4]Department of Biological Engineering, Massachusetts Institute of Technology, Cambridge, MA 02139

SUPPLEMENTARY FIGURE LEGENDS

Supplementary Figure S1. Monte Carlo sampling results for two-drug combinations on a thousand three-component tumor populations. Drug combination was optimized using an integer programming algorithm with the mathematical model described in Supplemental Text. Briefly, the optimization finds the optimal two-drug combination that minimizes the overall tumor heterogeneity, provided knowledge of the tumor composition and effects of single drugs on single subpopulations. The statistical sampling approach enables an examination of the frequency of a drug in optimal drug combinations, a characteristic that is independent on knowledge of an exact instance of tumor composition. (A) A uniform distribution of the subpopulations can be used for Monte Carlo sampling. (B) The resulting distribution of drugs in the two-drug combination optimized based on sampling from a subpopulation distribution in (A). (C) An alternative distribution of subpopulations, based on frequency of mutations observed in hematopoietic cancers (using COSMIC v67). (D) The resulting distribution of drugs in two-drug combination based on sampling from a subpopulation distribution in (C).

Supplementary Figure S2. Simulation results for two-drug combination on three-component tumor populations (all possible tumor compositions were enumerated with subpopulation proportions discretized

in 1% increments). Histogram shows the distribution of the difference in predicted efficacy (reported here as Δlog2RI) on each heterogeneous tumor between two two-drug combinations: one optimized based on considering the entire heterogeneous tumor versus one optimized based on considering just the heterogeneous tumor's predominant subpopulation.

Supplementary Figure S3. A schematic overview of the *in vitro* competition assay for single and combination drug treatments on individual shRNA population variants in heterogeneous lymphoma population. Parental *Eμ-myc; p19*$^{Arf-/-}$ lymphoma cells were infected with indicated retroviruses. For heterogeneous mixed population, the infected cells were sorted and mixed at indicated ratios prior to treatment. Single drug or drug combinations were dosed at concentrations to achieve a cumulative 80-90% cell death. Enrichment or depletion of the subpopulations was assessed using flow cytometry at 48 h.

Supplementary Figure S4. Bar graphs showing *in vitro* competition results for parental/shChk2/shBok, parental/shChk2/shBim and parental/shChk2/shBok/shChk2 *plus* shBok populations treated with four different drug combinations. Plots show enrichment/depletion of individual subpopulations. Each shRNA was tested in both Tomato-labeled MLT and GFP-labeled MLS vector to rule out vector-specific effects. No significant enrichment/depletion was observed with the MLS and MLT empty vectors alone.

Supplementary Figure S5. Rotated principal component analysis (PCA) of *in vitro* validation results. Optimal treatment moves the initial heterogeneous tumor state towards the objective – the minimization of clonal outgrowth.

Supplementary Figure S6. Representative *Ex vivo* whole mouse fluorescence imaging of vehicle-treated mice with mixed populations of parental/shChk2 (GFP-labeled)/shBok (Tomato-labeled) or empty vector control parental/mls (GFP-labeled)/mlt(Tomato-labeled) tumor cells. Mice were imaged 6 days following the emergence of palpable tumors. Mouse 4 with parental/shChk2/shBok was used for Fig. 3B.

Supplementary Figure S7. *Ex vivo* whole mouse fluorescence imaging followed by flow cytometry of individual tumors from mice with mixed populations of parental/shChk2 (GFP-labeled)/shBok (Tomato-labeled) or empty vector control parental/mls (GFP-labeled)/mlt (Tomato-labeled). Individual tumors were analyzed by flow cytometry and the adjacent pie charts show the proportion of the three tumor subpopulations.

Supplementary Figure S8. Determination of the optimal dose for individual drugs to ensure comparable therapeutic effect *in vivo* on control uninfected *Eμ-myc; p19*$^{Arf-/-}$ tumor from each component drug in the combination. (A) A diagram showing the transplanatation and treatment regimen. A total of 2 million uninfected cells were tail-vein injected into recipient mice. Mice were treated upon palpable tumor. (B) A list of optimized doses used for determining tumor-free survival. (C) A Kaplan-Meier curve showing tumor-free survival of mice treated with the doses indicated in B.

Supplementary Figure S9. Kaplan-Meier curves showing tumor-free survival of mice transplanted with (A) shChk2, (B) shBok or (C) parental homogeneous tumors, or (D-F) heterogeneous parental/shChk2/shBok tumors and treated with Vin/SAHA, IRT/CBL, or vehicle control. *P* value was calculated using a log-rank test.

Supplementary Figure S10. Kaplan-Meier curves showing tumor-free survival of mice transplanted with (A) shChk2, (B) shBok or (C) parental homogeneous tumors treated with Vin/SAHA or IRT/CBL. The data were derived from that in Supplementary Fig. S9, but now with days normalized to the median tumor-free survival of mice transplanted with homogeneous parental *Eμ-myc; p19*$^{Arf-/-}$ tumors. *P* value was calculated using a log-rank test.

Supplementary Figure S11. A ternary plot, generated using a descriptive model (see Supplementary Text), showing the comparison between Vin/SAHA and IRT/CBL in terms of absolute tumor-free survival in a shChk2/shBok/parental tumor at varying subpopulation proportions. Each white dot represents a tumor composition for which experiments were performed to determine the tumor-free survival of mice. Three of the dots are located at the corner of the ternary plot and represent homogeneous tumors that were used to generate the model. The position of the internal white dot approximates the heterogeneous tumor composition at the end of experiment in vehicle-treated mice.

Supplementary Figure S12. Theoretical tumor composition trajectories following multiple rounds of combination treatment with (A) Vin/SAHA or (B) IRT/CBL. Several initial tumor compositions, denoted with dotted circle in different colors, were selected as initials points for this model. Three rounds of treatments were simulated, with the tumor composition following each round of treatment denoted in a solid circle, and in increasing color intensity for each successive round (see Supplemental Text for details of mathematical model). Vin/SAHA had less selective pressure for outgrowth of subpopulations, whereas IRT/CBL strongly selected for shChk2, leading to its outgrowth after only a few rounds of treatment.

Supplementary Figure S1

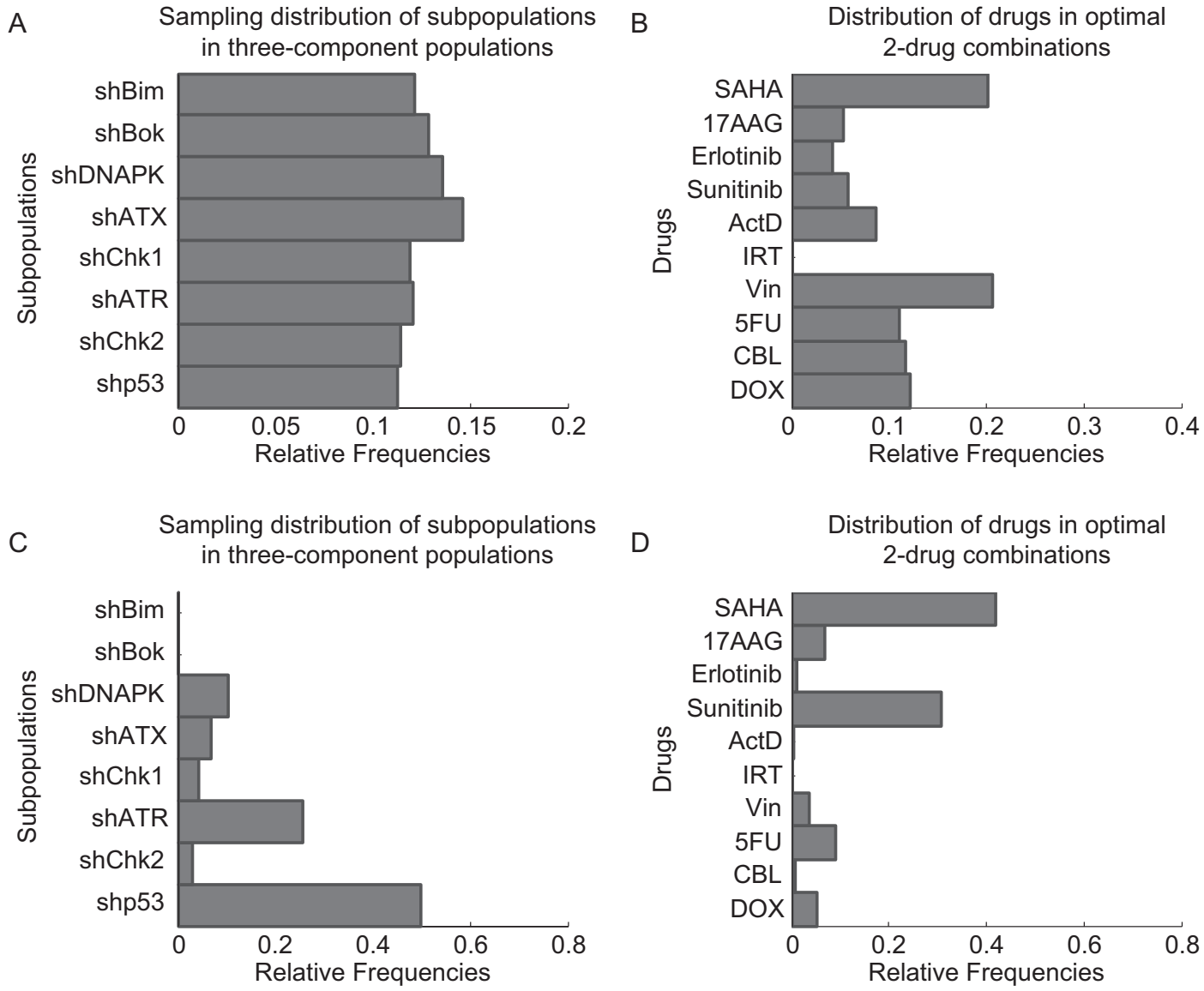

Supplementary Figure S2

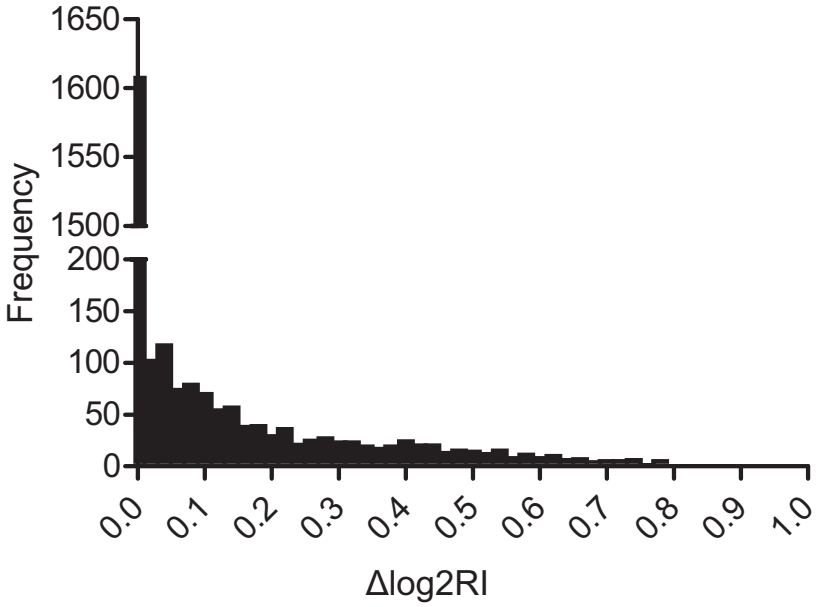

Supplementary Figure S3

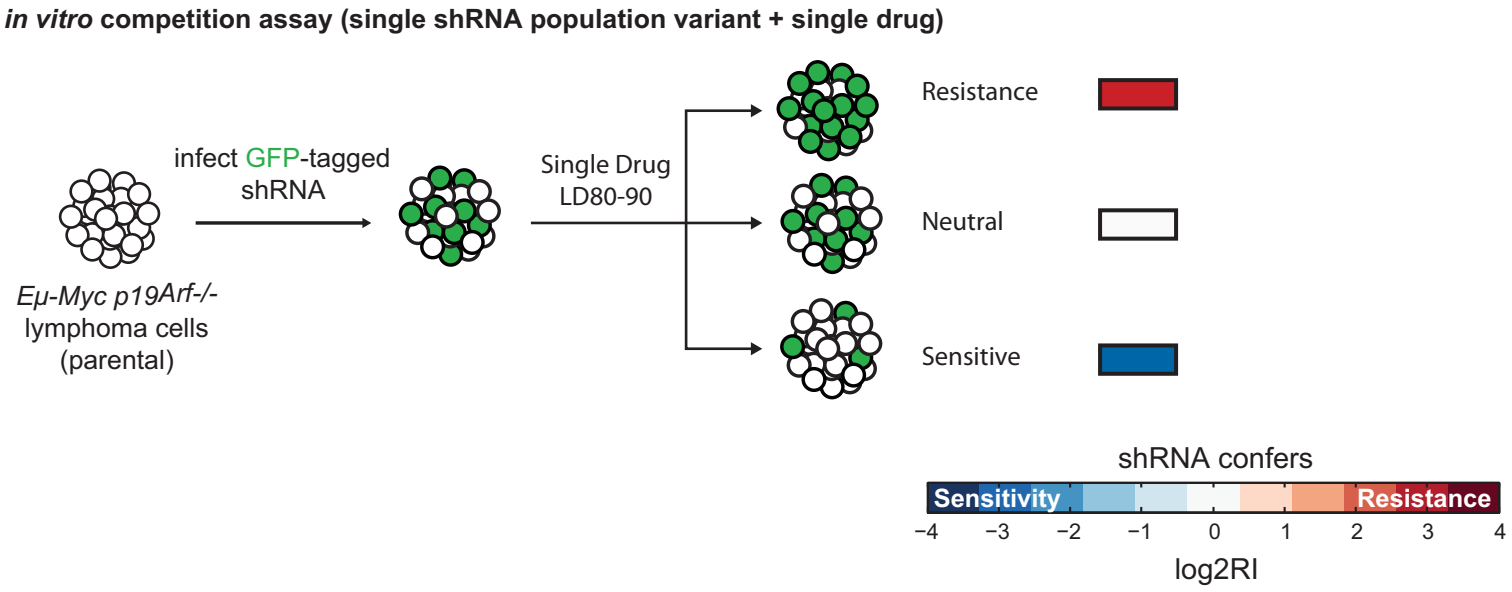

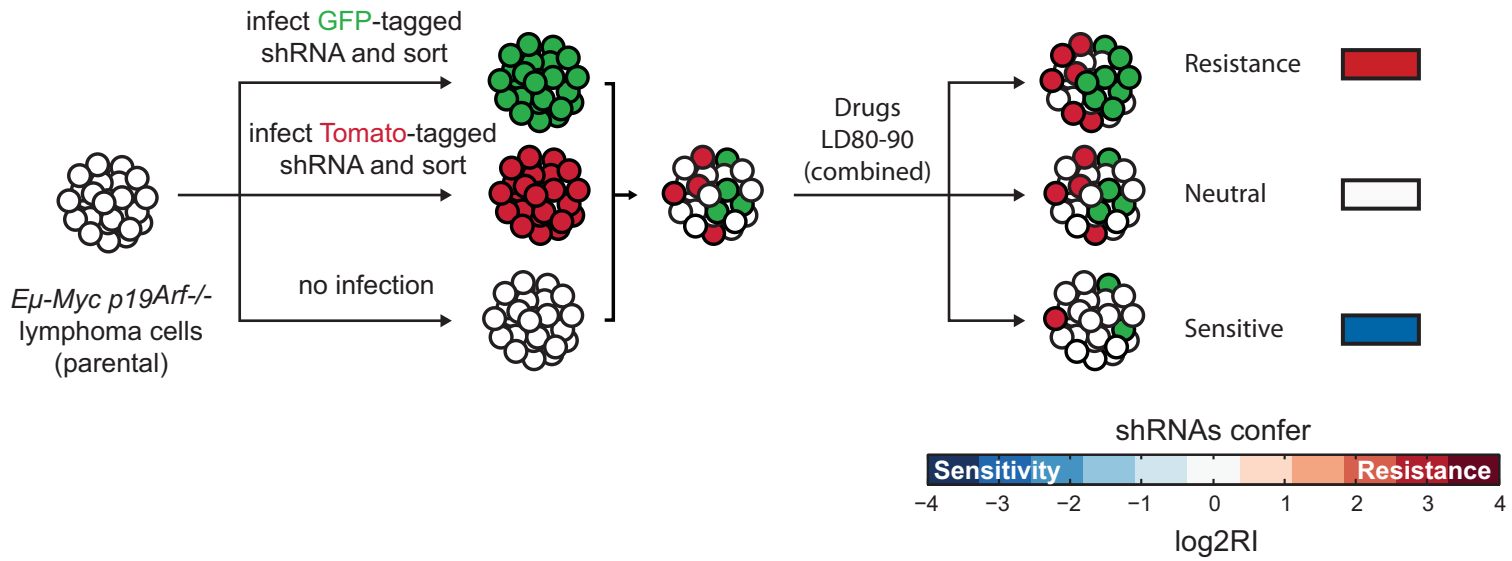

Supplementary Figure S4

shChk2/shBok/parental

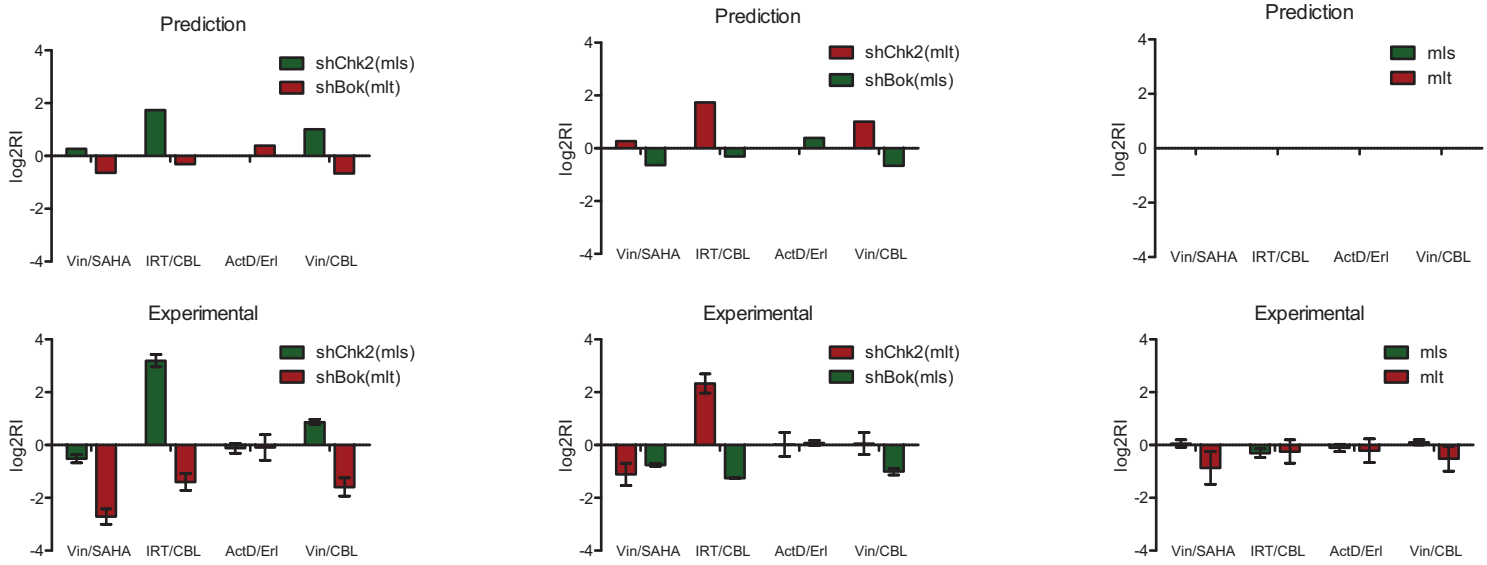

shChk2/shBim/parental

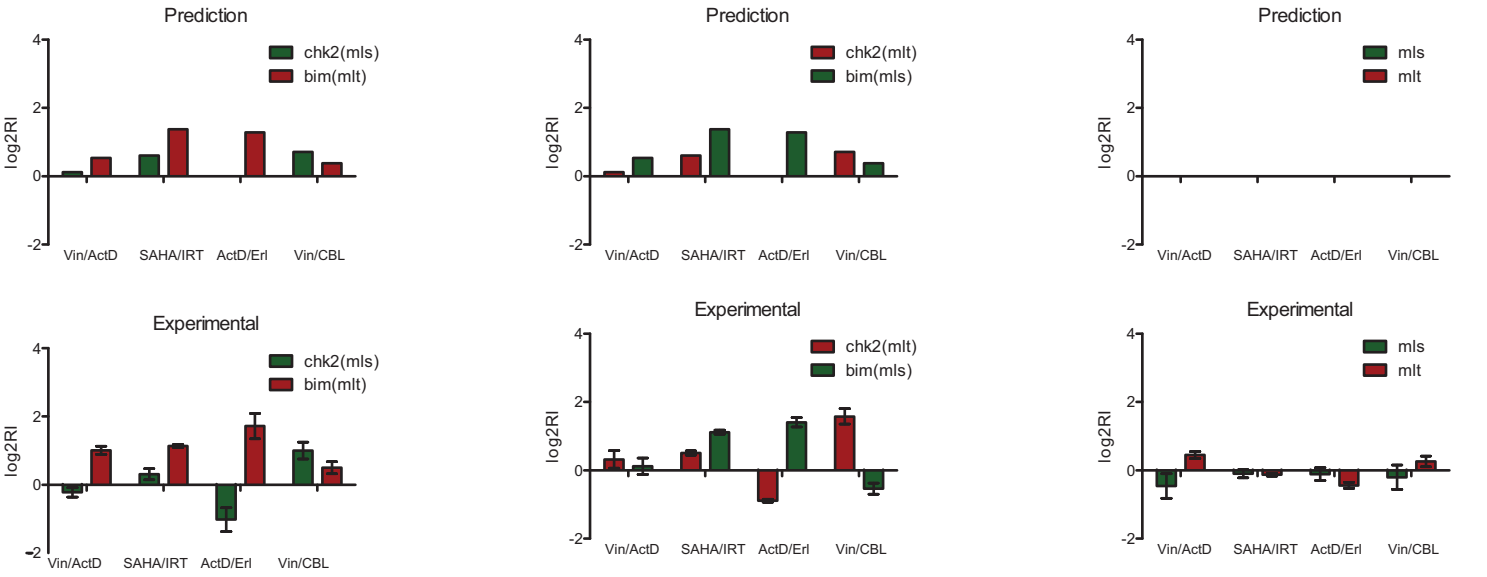

shChk2/shBok/shChk2&shBok/parental

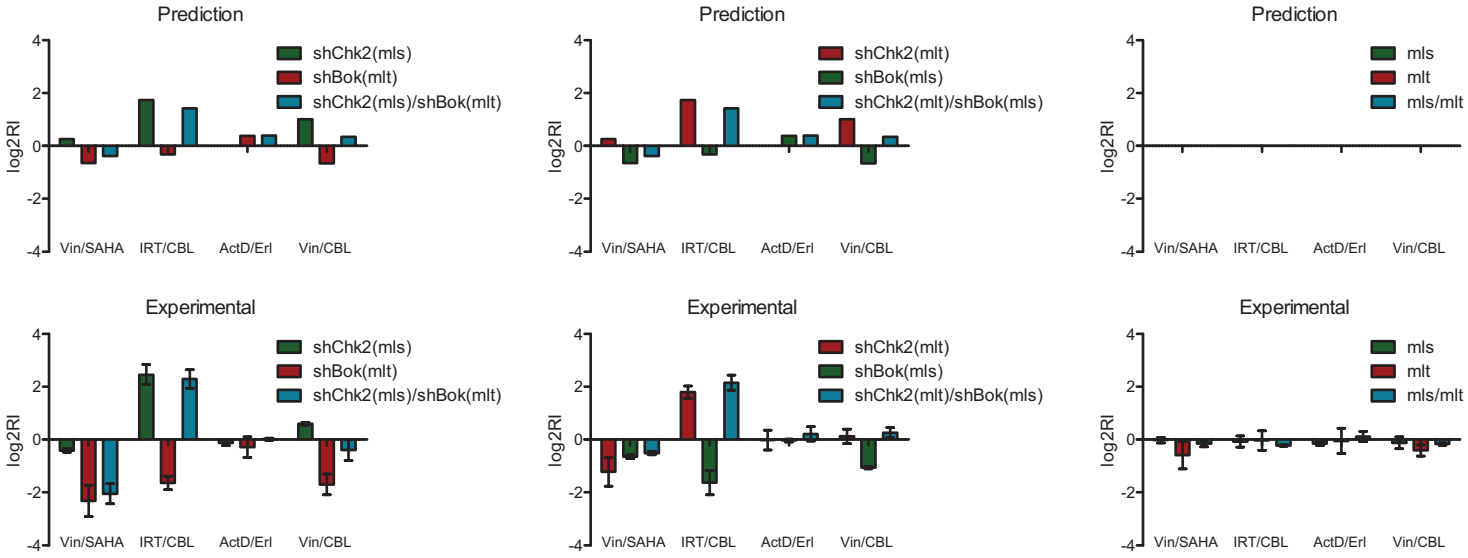

Supplementary Figure S5

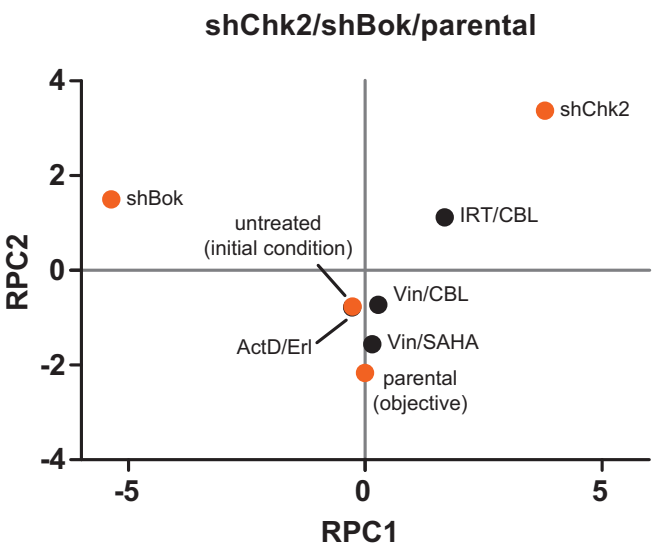

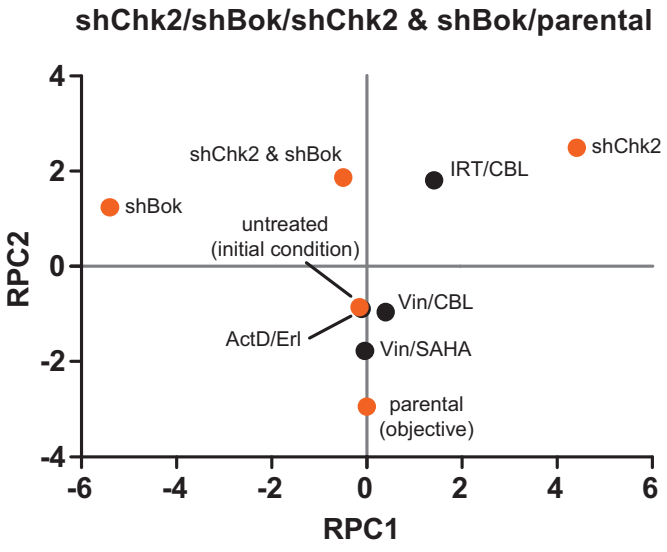

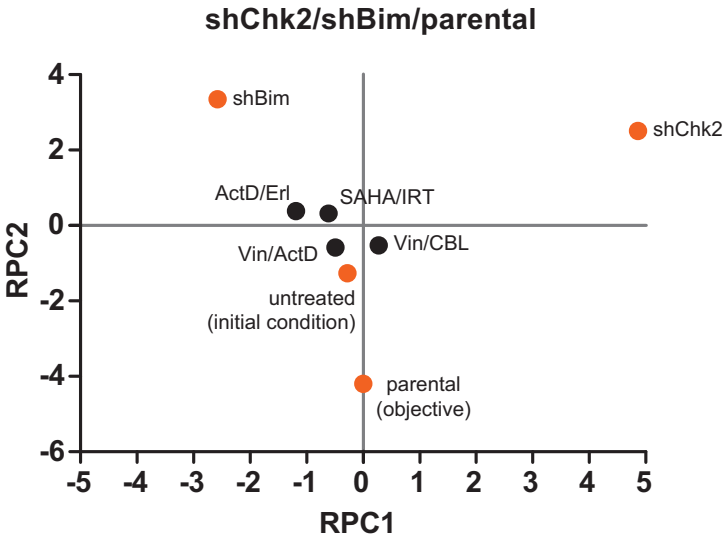

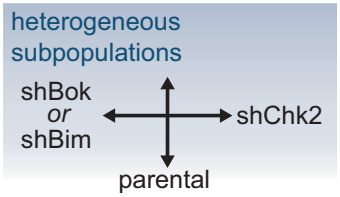

Supplementary Figure S6

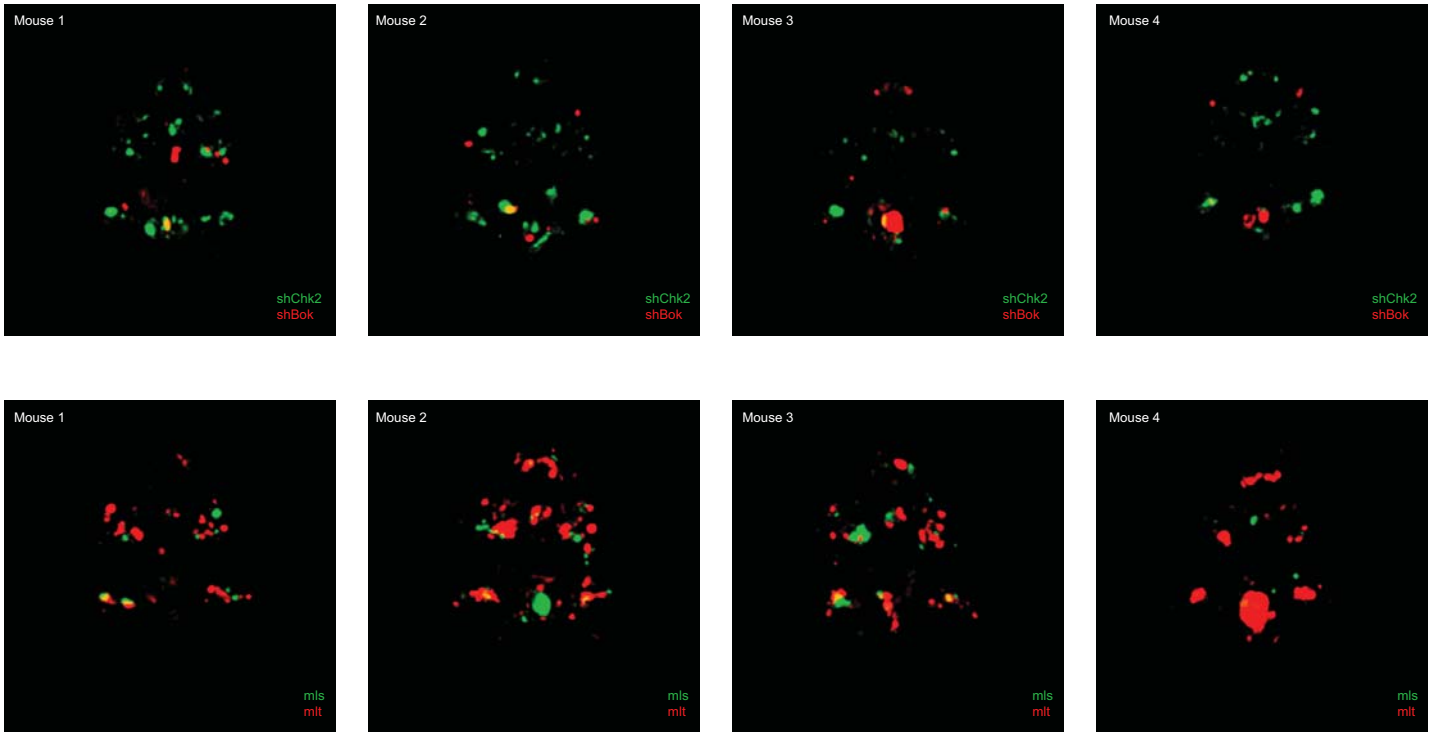

Supplementary Figure S7

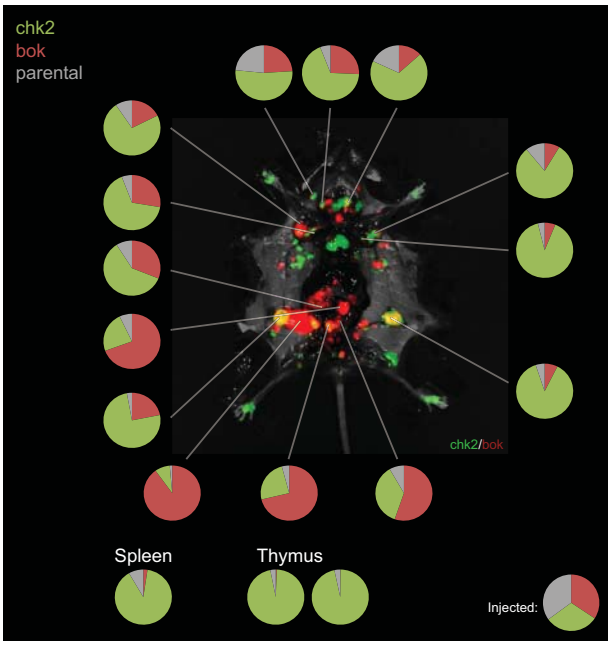

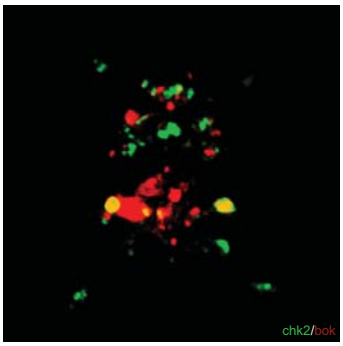

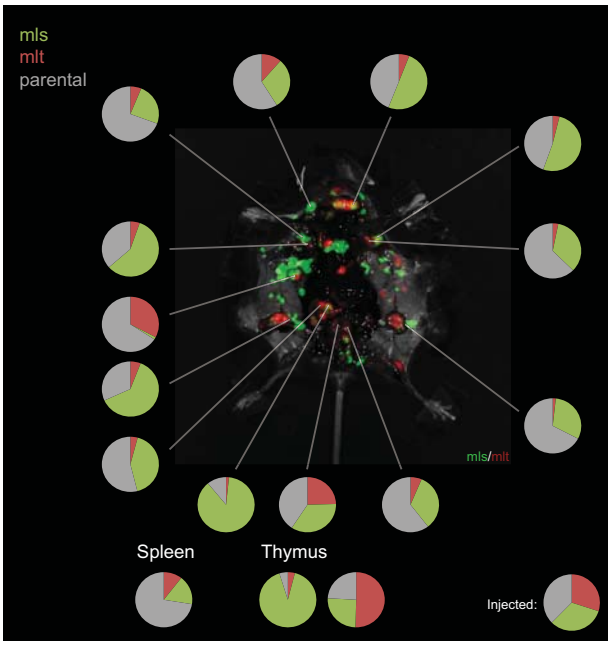

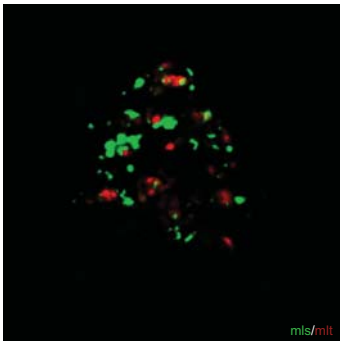

Supplementary Figure S8

A

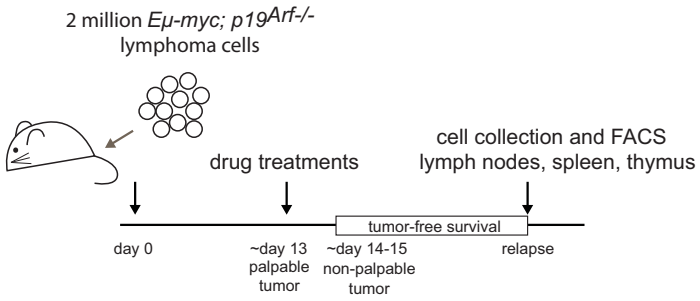

B

Drug name	Dose
Irinotecan (IRT)	120 mg/kg q1dx1
Vincristine (Vin)	1 mg/kg q1dx1
Chlorambucil (CBL)	10 mg/kg q1dx1
Vorinostat (SAHA)	300 mg/kg q1dx2 (d1,d3), 150 mg/kg q1dx2 (d2,d4)

C

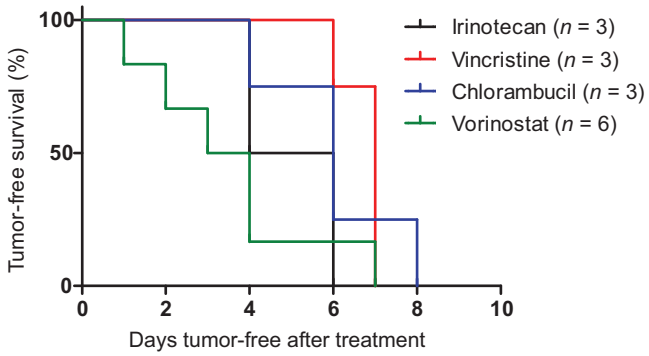

Supplementary Figure S9

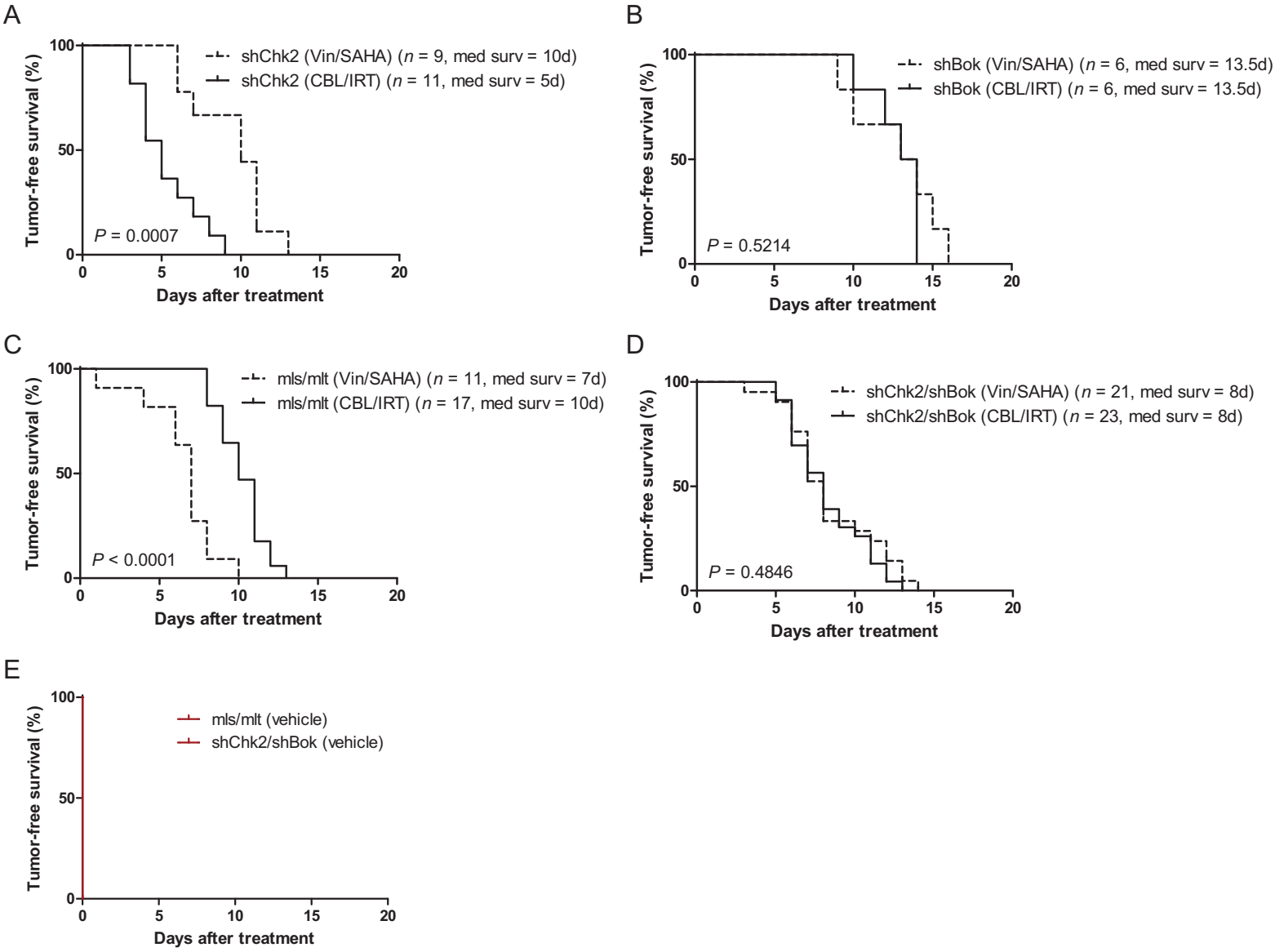

Supplementary Figure S10

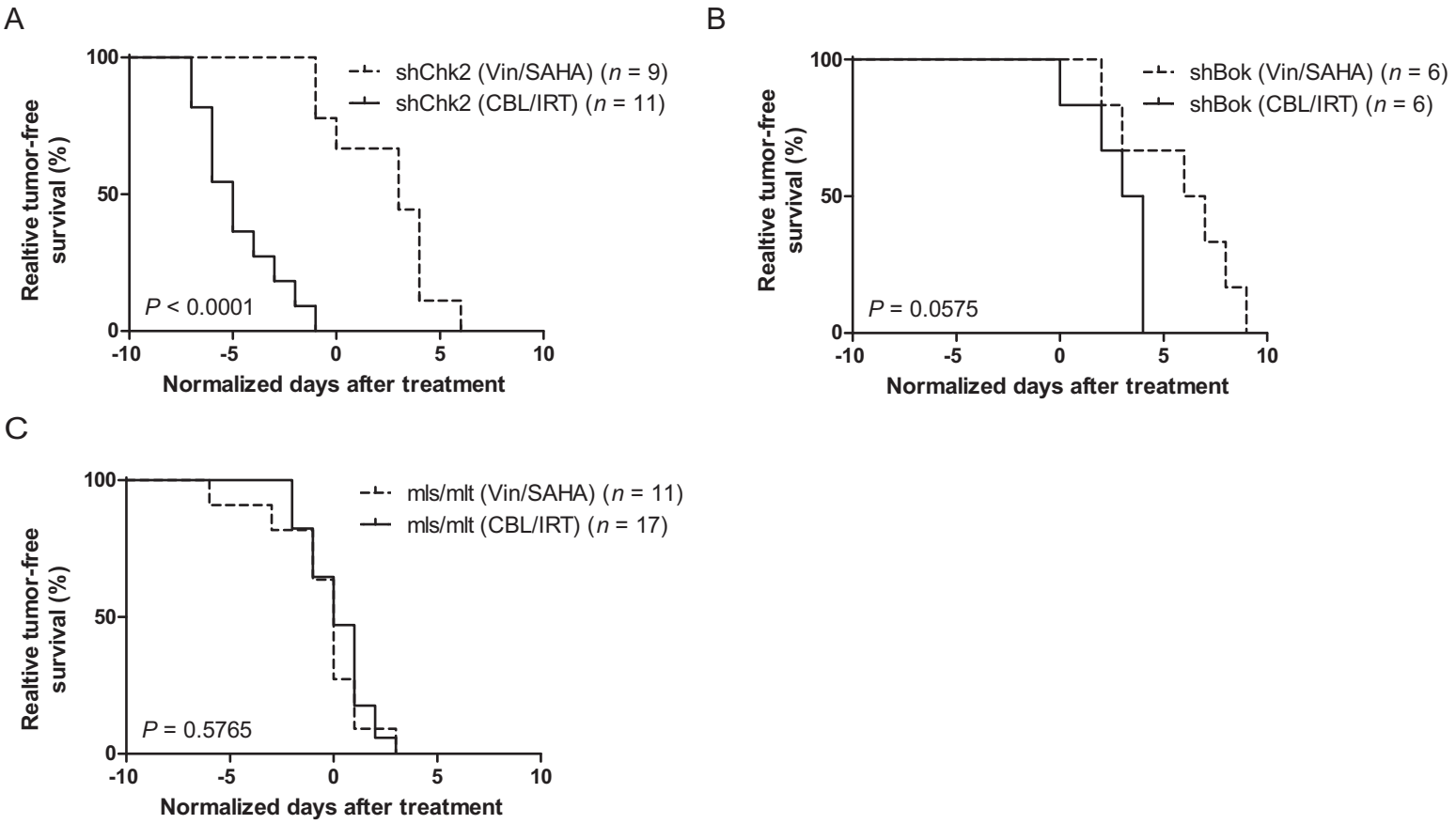

Supplementary Figure S11

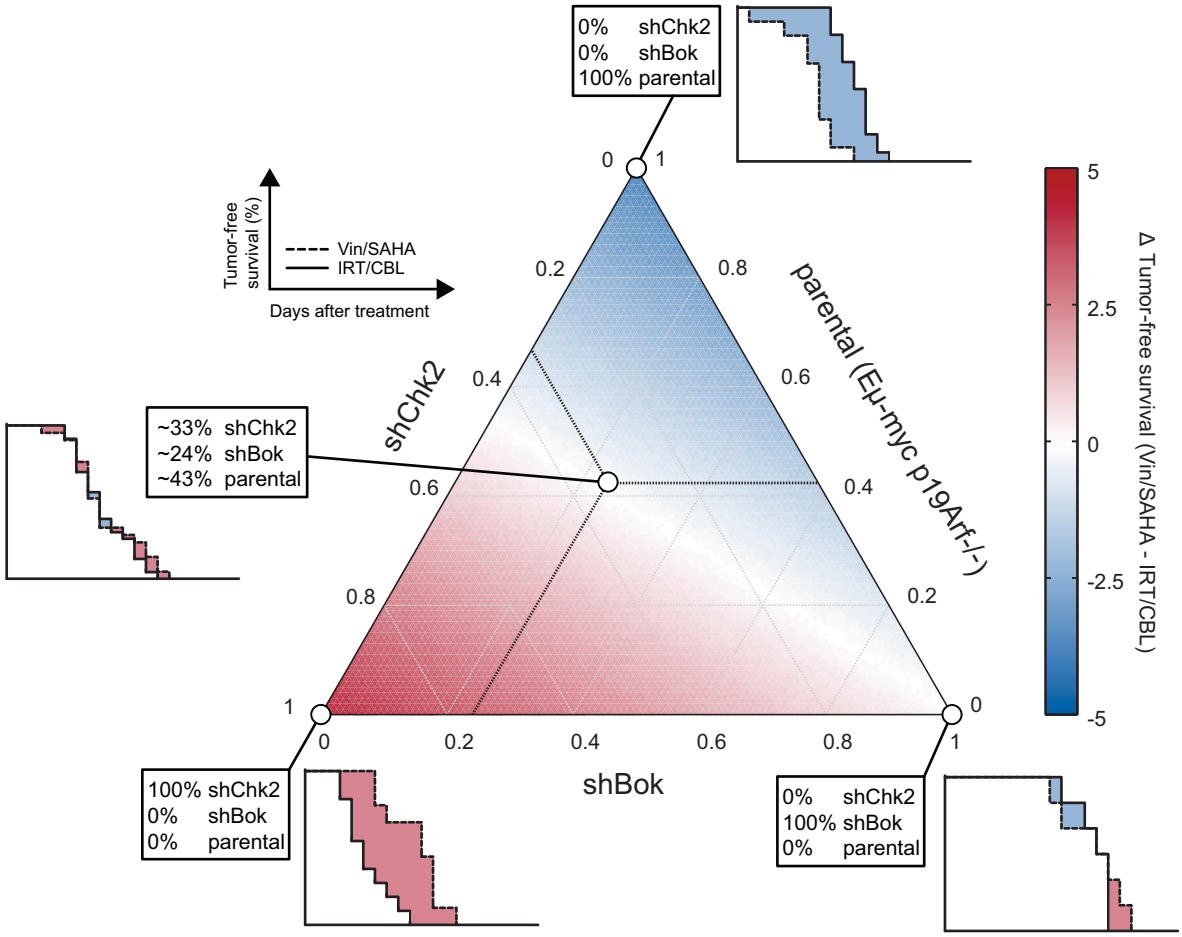

Supplementary Figure S12